Journal of Solid State Chemistry **167,** 160–167 (2002)
doi:10.1006/jssc.2002.9638

Phase Equilibrium in the System *Ln*–Mn–O IV. *Ln*=Sm at 1100°C

Kenzo Kitayama,[1] Minehito Kobayashi, and Takashi Kimoto

Department of Applied Chemistry and Biotechnology, Faculty of Engineering, Niigata Institute of Technology, Kashiwazaki, Niigata 945-1195, Japan

Received January 2, 2002; in revised form April 9, 2002; accepted May 3, 2002

Phase equilibrium in a Sm–Mn–O system has been established at 1100°C while changing the oxygen partial pressure from 0 to 13.00 in $-\log(P_{O_2}/\text{atm})$, and a phase diagram at 1100°C is presented for a Sm_2O_3–MnO–MnO_2 system. Under the experimental conditions, Sm_2O_3, MnO, Mn_3O_4, $SmMnO_3$, and $SmMn_2O_5$ phases are present at 1100°C, but Sm_2MnO_4, Mn_2O_3, and MnO_2 are unstable in the system. $LnMn_2O_5$- type phase is stable under the present experimental conditions differing from the previously reported La–Mn–O and Nd–Mn–O systems.

A wide range of nonstoichiometry has been found in the $SmMnO_3$ phase which coexisted with Sm_2O_3. X ranges from -0.010 at $\log P_{O_2} = -10.00$ to 0.098 at $\log P_{O_2} = 0$ in the molecular formula of $SmMnO_{3+X}$. The nonstoichiometry is represented by an equation, $N_O/N_{SmMnO_3} = 3.00\times10^{-4}(\log P_{O_2})^3 + 6.20\times10^{-3}(\log P_{O_2})^2 + 4.28\times10^{-2}(\log P_{O_2}) + 0.0979$, and the activities of the components in the solid solution are calculated using the equation. $SmMnO_3$ seems to vary in composition in the Sm_2O_3-rich or Sm_2O_3-poor side as it was with $LaMnO_3$. $SmMn_2O_5$ is slightly nonstoichiometric.

Lattice constants of $SmMnO_3$ made under different oxygen partial pressures and those of $SmMn_2O_5$ prepared in air were determined, along with spacings and relative intensities of $SmMn_2O_5$. Standard Gibbs energies of reactions shown in the system were calculated and compared with previously reported values.

Key Words: **phase equilibrium; thermogravimetry; Samarium-manganese oxide; Standard Gibbs energy change of reaction.**

INTRODUCTION

Many reports have been published on $LaMnO_3$ from the view of magnetic, electronic, and crystallographic properties (1–3).

Kamata *et al.* (4) reported that the perovskite phase $LaMnO_{3-\lambda}$ was revealed to have nonstoichiometry ranging from 2.947 to 3.079 under the oxygen partial pressure below $\log(P_{O_2}/\text{atm}) = 0$ at 1200°C, and Nakamura *et al.* (5) reported that the stability limit of the perovskite phases expressed in terms of $-\log(P_{O_2}/\text{bar})$ for $LaMnO_3$ is 15.05. Solid-state equilibrium relations were studied in the region of the La–Mn–O system bounded by $LaMnO_3$, MnO, and La_2O_3, and in the temperature range 900–1380°C the defective perovskite $LaMnO_{3-\lambda}$ coexist directly in equilibrium with lanthanum oxide and manganous oxide (6). Van Roosmalen *et al.* (7) presented the pseudobinary La_2O_3–Mn_2O_3 phase diagram in air and concluded that the perovskite-type $LaMnO_{3+\delta}$ solid solution can be formed with excess La as well as with excess Mn.

Recently, phase equilibria in the *Ln*–Mn–O (*Ln* = La (8), Nd (9), and Gd (10)) systems have been established at 1100°C. It has been found that not only $LnMnO_3$ type was stable in La–Mn–O and Nd–Mn–O systems as the ternary compound under the experimental conditions, but $GdMn_2O_5$ was also stable in addition to $GdMnO_3$ in Gd–Mn–O system under the same experimental conditions. By this time, two types of phase diagram in *Ln*–Mn–O system have been found at 1100°C. That is: (1) only $LnMnO_3$ is present as the ternary compound and (2) $LnMnO_3$ and $LnMn_2O_5$ compounds are present as the ternary compound.

$LnMn_2O_5$-type phase has already been reported to be stable in the *Ln*–Mn–O system. A compound $LnMn_2O_5$ crystallize in the orthorhombic, *Pbam* (11). Decomposition temperatures of $LnMn_2O_5$ (*Ln* = Pr, Nd, Sm, Eu, Gd, Tb, Dy, Ho, Er, Tm, Yb, and Y) were measured by thermogravimetry and differential thermal analysis under various oxygen partial pressures and the decomposition reactions were confirmed by identifying the decomposition products (12). By neutron diffraction method, the magnetic ordering of the rare-earth moments are studied at low temperatures in TMn_2O_5 (T = Nd, Tb, Er) and the results were discussed on the basis of a polarization of the rare earths by the molecular field due to the manganese spins (13). RMn_2O_5 (R = La, Pr, Nd, Sm, Eu, Tb, Ho, Er) have been prepared in polycrystalline form by a citrate technique, and excepting the Sm and Eu phases, structu-

[1] Correspondence should be addressed. Fax: 0257-22-8142. E-mail: kitayama@acb.niit.ac.jp.

0022-4596/02 $35.00

rally studied by high-resolution neutron powder diffraction. All the materials are isostructural (space group *Pbam*, $Z = 4$) and the magnetic properties strongly depend on the nature of R (14). The magnetoelectric effect of rare-earth oxides $R\mathrm{Mn_2O_5}$ has been studied by a quasistatic magnetoelectric method for the purpose of determining whether linear magnetoelectric effect was present or not (15).

As is well known, in the Mn–O system there are four stable oxide-phases, MnO, $\mathrm{Mn_3O_4}$, $\mathrm{Mn_2O_3}$, and $\mathrm{MnO_2}$. However, only two-oxide phases, MnO and $\mathrm{Mn_3O_4}$, are stable under the present experimental conditions (8–10), and the oxygen partial pressure in equilibrium with MnO and $\mathrm{Mn_3O_4}$ has been found to be -5.40 in $\log(P_{\mathrm{O_2}}(\mathrm{atm}))$ (8).

In the Sm–Mn–O system, $\mathrm{SmMnO_3}$ and $\mathrm{SmMn_2O_5}$ ternary phases are stable. But the phase equilibrium in the Sm–Mn–O system has not been established even at high temperatures.

In consideration of the above circumstances, the objectives of the present study are: (1) to establish a detailed phase diagram of the Sm–Mn–O system at 1100°C as a function of the oxygen partial pressure and to ascertain the nonstoichiometric range of $\mathrm{SmMnO_3}$ and $\mathrm{SmMn_2O_5}$, (2) to determine the thermochemical properties based on the established phase diagram, and (3) to obtain the crystallographic data of $\mathrm{SmMn_2O_5}$ if it would be stable under the present experimental conditions.

EXPERIMENTAL

Analytical-grade $\mathrm{Sm_2O_3}$ (99.9%) and MnO (99.9%) were used as starting materials. MnO was dried by heating at 110°C in air, and $\mathrm{Sm_2O_3}$ was dried at 1100°C. Mixtures with desired ratios of $\mathrm{Sm_2O_3}$/MnO were prepared by mixing in an agate mortar with repeated intermittent calcination by solid reaction at 1100°C. This procedure is the same as that described previously (16).

Mixed gases of $\mathrm{CO_2}$ and $\mathrm{H_2}$, and $\mathrm{CO_2}$ and $\mathrm{O_2}$, and single-component gases of $\mathrm{O_2}$ and $\mathrm{CO_2}$ were used to obtain the oxygen partial pressures in the present experiment.

The apparatus and procedures for controlling the oxygen partial pressure, maintaining constant temperature, the method of thermogravimetry, and the criterion for the establishment of equilibrium were the same as those described in the previous paper (16). Briefly, to ensure equilibrium, the equilibrated point of each sample at a given oxygen partial pressure was determined from both sides of the reaction, that is, from low oxygen partial pressures to high oxygen partial pressures, and vice versa. The oxygen partial pressure in equilibrium was determined as follows. As is known from the Gibbs phase rule, the freedom in a three-phrase regions is zero under present experimental conditions. That is, the oxygen partial pressure in equilibrium is invariable and defined by the experimental temperature and pressure conditions. For example, for $0.60\mathrm{Sm_2O_3}/0.40\mathrm{MnO}$ (Fig. 1a), $\log P_{\mathrm{O_2}} = 10.00$ is invariable under given temperature and pressure conditions. The exact value is obtained through experiment: to determine the oxygen partial pressure in equilibrium, the weight of sample on a balance is measured while the sample is taken through the three phase regions by controlling the $\mathrm{CO_2}/\mathrm{H_2}$ ratio. If the stabilized oxygen partial pressure is higher than the oxygen partial pressure in equilibrium, the sample on the balance will become heavier, and vice versa. Repeating the procedure, the oxygen partial pressure will approach that in equilibrium.

Schematics of the balance, furnace, and gas mixer are given in the previous report (17). The furnace is installed vertically and employs as its heating element a mullite tube wound with Pt 60%–Rh 40% alloy wire. Mixed gases pass from the bottom of the furnace to the top.

The identification of phases and the determination of lattice constants were performed using an X-ray diffractometer (Rint 2500, Rigaku) with Ni-filtered Cu$K\alpha$ radiation. A specimen of silicon was used to calibrate 2θ as an external standard.

RESULTS AND DISCUSSIONS

Sm_2O_3–MnO–MnO_2 system

The Mn–O system at 1100°C related to the present phase diagram has been described in previous works (8, 9). Here, the results are briefly described as follows; the MnO and $\mathrm{Mn_3O_4}$ phases are stable, and MnO is nonstoichiometric, whereas $\mathrm{Mn_3O_4}$ is stoichiometric. The oxygen partial pressure in equilibrium with MnO and $\mathrm{Mn_3O_4}$ is -5.40 in $\log(P_{\mathrm{O_2}}(\mathrm{atm}))$.

Six samples, having $\mathrm{Sm_2O_3}$/MnO mole ratios of 0.6/0.4, 0.4/0.6, 0.3/0.7, 0.25/0.75, 0.15/0.85, and 0.1/0.9, were prepared for thermogravimetry. Figure 1 shows the oxygen partial pressure $-\log(P_{\mathrm{O_2}}(\mathrm{atm}))$, versus the weight changes, $W_{\mathrm{O_2}}/W_{\mathrm{T}}$, for three representative samples: 0.6/0.4 (Fig. 1a), 0.25/0.75 (Fig. 1b), and 0.15/0.85 (Fig. 1c). Here, $W_{\mathrm{O_2}}$ is the weight increase of a sample from the reference weight at $\log(P_{\mathrm{O_2}}(\mathrm{atm})) = -13.00$, at which $\mathrm{Sm_2O_3}$ and MnO are stable, and W_T is the total weight gain from reference state to the state at 1 atm $\mathrm{O_2}$, at which $\mathrm{Sm_2O_3}$ and $\mathrm{SmMnO_3}$, or $\mathrm{SmMnO_3}$ and $\mathrm{SmMn_2O_5}$ or $\mathrm{SmMn_2O_5}$ and $\mathrm{Mn_3O_4}$ are stable, depending on the overall composition of the samples. As is evident from Fig. 1, weight breaks are found at 10.00, 5.40, and 1.55 in $-\log(P_{\mathrm{O_2}}(\mathrm{atm}))$. These values correspond to the oxygen partial pressure in equilibrium with the three solid phases, $\mathrm{Sm_2O_3} + \mathrm{SmMnO_3} + \mathrm{MnO}$, $\mathrm{SmMnO_3} + \mathrm{MnO} + \mathrm{Mn_3O_4}$, or $\mathrm{SmMnO_3} + \mathrm{Mn_3O_4} + \mathrm{SmMn_2O_5}$, respectively.

Table 1 shows the results of identified phases in the Sm–Mn–O system, together with the experimental

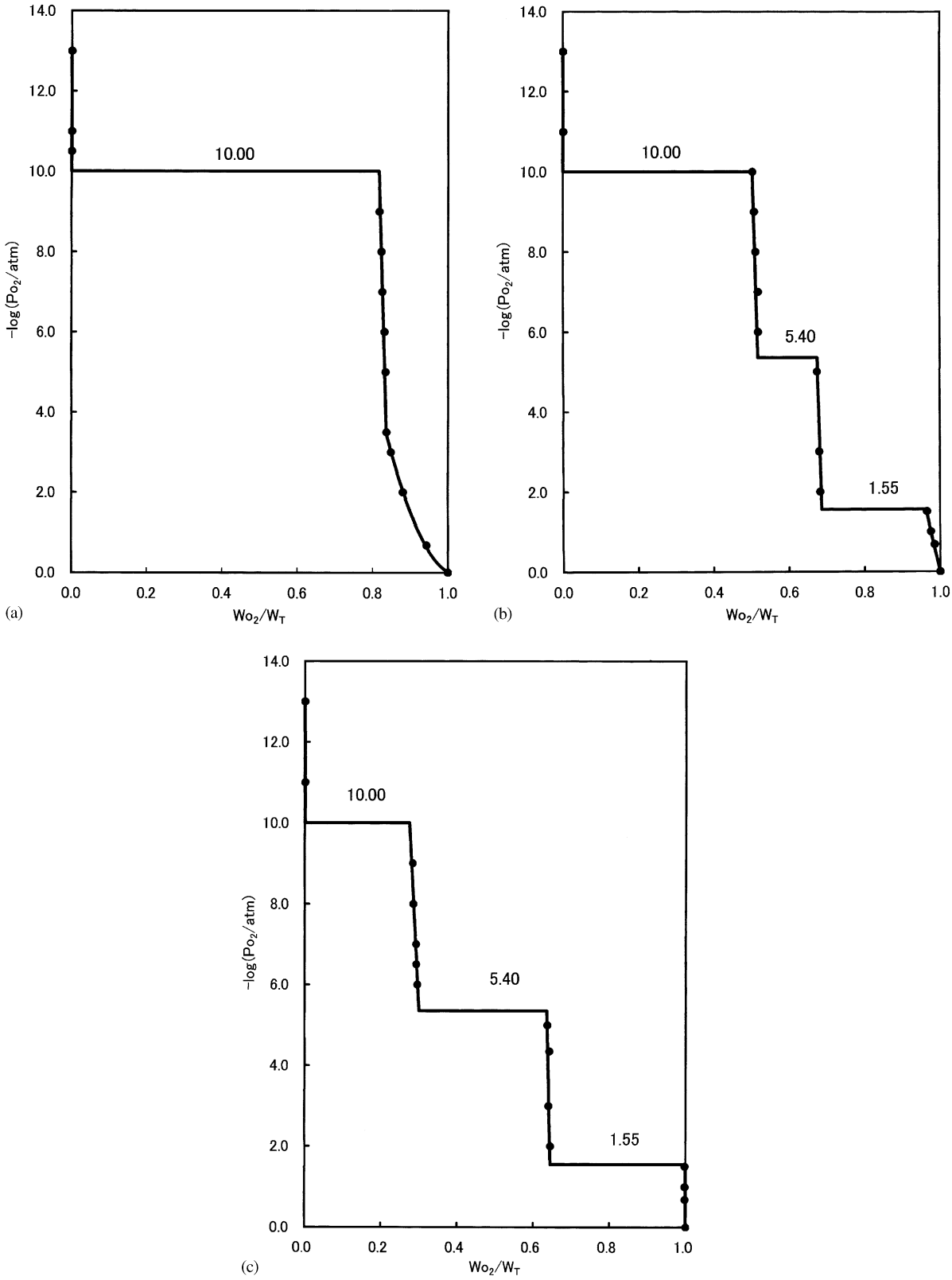

FIG. 1. Relationships between the oxygen partial pressure, $\log(P_{O_2}(\text{atm}))$, and the weight change of the samples, W_{O_2}/W_T. (a) $Sm_2O_3/MnO = 0.60/0.40$, (b) $Sm_2O_3/MnO = 0.25/0.75$, and (c) $Sm_2O_3/MnO = 0.15/0.85$.

TABLE 1
Identification of Phase

Sample (mol ratio)				
Sm_2O_3	MnO	$-\log(P_{O_2}(atm))$	Time (h)	Phase
0.6	0.4	13.00	8	$Sm_2O_3 + MnO$
		10.50	8	$Sm_2O_3 + MnO$
		9.00	13	$Sm_2O_3 + SmMnO_3$
		0.68	14.5	$Sm_2O_3 + SmMnO_3$
0.4	0.6	13.00	8	$Sm_2O_3 + MnO$
		10.50	8	$Sm_2O_3 + MnO$
		9.00	13	$Sm_2O_3 + SmMnO_3$
		0.68	14.5	$Sm_2O_3 + SmMnO_3$
0.25	0.75	13.00	8	$Sm_2O_3 + MnO$
		10.50	8	$Sm_2O_3 + MnO$
		9.00	13	$SmMnO_3 + MnO$
		6.00	16	$SmMnO_3 + MnO$
		5.00	18.5	$SmMnO_3 + Mn_3O_4$
		2.00	19.5	$SmMnO_3 + Mn_3O_4$
		0.68	120	$SmMnO_3 + SmMn_2O_5$
0.1	0.9	13.00	8	$Sm_2O_3 + MnO$
		10.50	8	$Sm_2O_3 + MnO$
		9.00	13	$SmMnO_3 + MnO$
		6.00	16	$SmMnO_3 + MnO$
		5.00	18.5	$SmMn_2O_5 + Mn_3O_4$
		2.00	19.5	$SmMn_2O_3 + Mn_3O_4$
		0.68	120	$SmMn_2O_5 + Mn_3O_4$
0.0	1.0	13.00	6	MnO
		5.00	46.5	Mn_3O_4
		0.68	46.5	Mn_3O_4

conditions. Samples of about 500 mg were prepared for the identification of phases by means of the quenching method. Five phases, Sm_2O_3, MnO, Mn_3O_4, $SmMnO_3$, and $SmMn_2O_5$ were found to be stable by X-ray diffractometer and were found to be stable under the experimental conditions.

From the above results of thermogravimetry and phase identification, a phase diagram was drawn and shown in Fig. 2 as a Sm_2O_3–MnO–MnO_2 system, although MnO_2 is not stable under the experimental conditions. The numerical values in the three solid fields in Fig. 2 are the values of $-\log P_{O_2}$ in equilibrium with the three solid phases described above, and those found in the two-phase regions are also the oxygen partial pressures in $\log P_{O_2}$, which are shown by dotted lines. Nonstoichiometry of MnO is ascertained by the results of thermogravimetry of the other two samples, shown in Figs. 1b and 1c. That is, nonstoichiometry is represented by slight changes in the composition in the range from 10.00 to 5.40 in $-\log P_{O_2}$.

$SmMnO_3$ has a large nonstoichiometric composition within the range from -10.00 to 0 in $\log P_{O_2}$. Fig. 3 shows the relationship between the oxygen partial pressure and the composition of the $SmMnO_3$ solid solution, which coexisted with Sm_2O_3. This curve is represented by an equation: $N_O/N_{SmMnO_3} = 3.00 \times 10^{-4}(\log P_{O_2})^3 + 6.20 \times 10^{-3}(\log P_{O_2})^2 + 4.28 \times (\log Po2) + 0.0979$. Here, N_O and N_{SmMnO_3} represent the mole fraction of oxygen and $SmMnO_3$ in the solid solution. This equation can be solved to show that samarium–manganese perovskite would be stoichiometric at -7.00 in $\log(P_{O_2}(atm))$. As shown in Fig. 2, the composition of the $SmMnO_3$ solid solutions on the Sm_2O_3-rich side and that on Sm_2O_3-poor side are not the same. This suggested that the region exhibits some width with respect to the direction between the Sm_2O_3 side and the Mn_3O_4. Van Roosmalen *et al.* (7) reported that a perovskite-type $LaMnO_{3+\delta}$ solid solution can be formed with excess La as well as with excess Mn. The same phenomenon was also found in the other *Ln*–Mn–O systems (8–10). However, its width has not been detected by the present experimental techniques. The curved line of $\log P_{O_2}$ might be drawn from Gibb's phase rule, that is, one-phase region, $SmMnO_3$, of a three-component system has two degrees of freedom. Consequently, the oxygen partial pressure lines in one-phase area could be curved if its phase would be area.

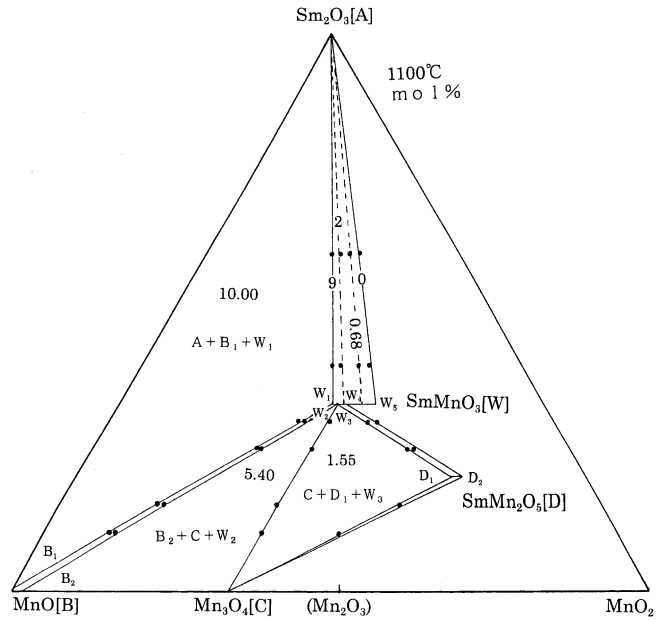

FIG. 2. Phase equilibrium in the Sm_2O_3–MnO–MnO_2 system at 1100°C. Numerical values in the three-phase regions are the oxygen partial pressures in $-\log(P_{O_2}(atm))$ in equilibrium with three solid phases, which are shown in the regions. Dotted lines in two-phase regions are also the oxygen partial pressures indicated by the lines. Abbreviations are the same as those used in Table 2.

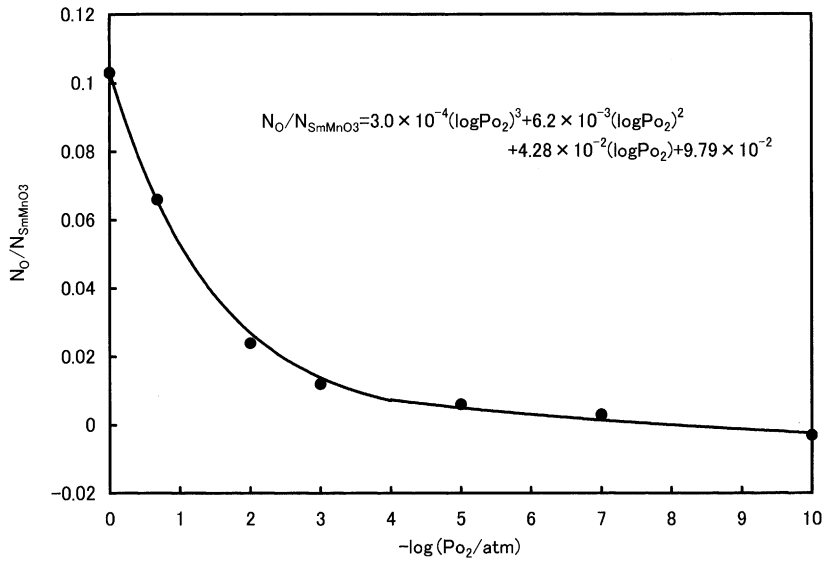

FIG. 3. Oxygen partial pressure, $-\log(P_{O_2}(\text{atm}))$ versus the composition of $SmMnO_3$ solid solution, $N_O/N_{SmMn_2O_5}$.

Compositions, symbols, stability ranges in oxygen partial pressures of compounds and activities of components in the solid solutions are tabulated in Table 2.

Lattice constants of $SmMnO_3$ perovskite were determined as orthorhombic at 9.00, 5.00, and 0.68 in $-\log P_{O_2}$ from samples of Sm_2O_3/MnO at mole ratios of 0.4/0.6 and 0.25/0.75. These samples were selected for their ability to coexist with Sm_2O_3 or Mn_3O_4. The results are tabulated in Table 3 together with the previously reported values. Slight differences were found in the lattice constants and the volume among Sm_2O_3 coexisted samples, depending on the oxygen partial pressure. The samples prepared in 0.68 in $-\log P_{O_2}$ are of smaller volume than those prepared at 9.00 in $-\log P_{O_2}$. This could stem from the difference in the ionic radii of Mn^{3+} 0.72 Å and Mn^{4+} 0.68 Å, with each having a coordination number 6, respectively (21). The content of Mn^{4+} in the solid solution prepared in $\log P_{O_2} = -0.68$ must be more than that prepared in $\log P_{O_2} = -9.00$ resulting from Fig. 2.

TABLE 2
Compositions, Stability Ranges in Oxygen Partial Pressures, and Activities of Components in Solid Solutions

Component	Compositions	$-\log(P_{O_2}(\text{atm}))$	$\log a$	Symbol
MnO	$MnO_{1.000}$	13.00–10.00	0	B_1
	$MnO_{1.02}$	5.40	-9.58×10^{-3}	B_2
$SmMnO_3$	$SmMnO_{2.997}$	10.00	0	W_1
	$SmMnO_{3.012}$	5.40	-5.31×10^{-3}	W_2
	$SmMnO_{3.039}$	1.55	-2.40×10^{-2}	W_3
$SmMn_2O_5$	$SmMn_2O_{4.92}$	1.55	0	D_1
	$SmMn_2O_5$	0.00	-1.13×10^{-2}	D_2

Note. $(N_O/N_{SmMnO_3}) = 0.0003(\log P_{O_2})^3 + 0.0062(\log P_{O_2})^2 + 0.0428(\log P_{O_2}) + 0.0979$
$(N_O/N_{SmMn_2O_5}) = -0.0156(\log P_{O_2})^2 + 0.0291(\log P_{O_2}) + 0.0011.$

Compound, $SmMn_2O_5$

In the Sm–Mn–O system $SmMn_2O_5$ is stable as a ternary compound unlike the La and Nd systems. Preparing the compound by means of the usual solid-state reaction is very difficult, on account of the slow reaction rate. It takes more than 3 days in air to prepare $SmMn_2O_5$ by heating a mixture of Sm_2O_3 and MnO at even 1100°C.

The compound have nonstoichiometric composition, and the relationship between the oxygen partial pressure and the composition of $SmMn_2O_5$ solid solution, $N_O/N_{SmMn_2O_5}$, is shown with an equation, $N_O/N_{SmMn_2O_5} = -0.0156(\log P_{O_2})^2 + 0.0291(\log P_{O_2}) + 0.0011$. Lattice constants and spacings were determined based upon the data of $NdMn_2O_5$ (22) because the ionic radius of Nd is close to that of Sm. Results of lattice constant are shown in Table 4 together with previously reported values. The determined spacings and relative intensities are also shown in Table 5. Observed d(obs.) values are in good agreement with calculated d(cal.) values.

Standard Gibbs Energy Change of Reaction

On the basis of the established phase diagram, the standard Gibbs energy changes of reactions in Table 4 were determined by the equation, $\Delta G^\circ = -RT\ln K$. Here R is the gas constant, T the absolute temperature, and K the equilibrium constant of the reaction. The standard state of the activities of components in the solid solutions can be

TABLE 3
Lattice Constants of Quenched $SmMnO_3$

Sample (mol ratio)								
Sm_2O_3	MnO	$-\log(P_{O_2}(\text{atm}))$	Time (h)	a (Å)	b (Å)	c (Å)	V (Å)^3	Coexistent phase
0.4	0.6	9.0	13	5.363 (5)	5.842 (5)	7.481 (9)	234.4 (4)	Sm_2O_3
		5.0	23.5	5.362 (4)	5.843 (4)	7.474 (6)	234.2 (3)	Sm_2O_3
		0.68	14.5	5.365 (6)	5.796 (5)	7.493 (9)	233.0 (4)	Sm_2O_3
0.25	0.75	9.0	13	5.358 (3)	5.849 (3)	7.474 (4)	234.2 (2)	MnO
		5.0	18.5	5.350 (3)	5.802 (3)	7.481 (3)	232.2 (2)	Mn_3O_4
		0.68	120	5.353 (5)	5.796 (7)	7.847 (10)	232.3 (5)	$SmMn_2O_5$
Ref. (18)		—	—	5.358	5.825	7.483	—	—
Ref. (19)		—	—	5.376	5.788	7.520	—	—
Ref. (20)		—	—	5.357	5.825	7.482	—	—

arbitrarily chosen for each solid solution and is indicated as $\log a_i = 0$ in Table 2.

Calculated values for reactions which appear in the phase diagram is shown in Table 6. The ΔG° value for reaction (1) is -65.6 kJ/mol. This value is larger than those of -85.3 for $LaMnO_3$, and -71.3 for $NdMnO_3$, and is smaller than -62.2 for $GdMnO_3$ as expected from the oxygen partial pressure in equilibrium.

For reaction (2), the oxygen partial pressure in equilibrium is -1.55 in $\log(P_{O_2}/\text{atm})$ and $\Delta G^\circ = 13.7$ kJ/mol. As is shown in Fig. 2, $SmMn_2O_5$ is nonstoichiometric. Therefore, taking the activity of component of $SmMn_2O_5$ at the composition D_1 to be unity, the ΔG° value was calculated. Satoh *et al.* (12) reported the oxygen partial pressure -1.54 in $\log P_{O_2}$ for the reaction by means of emf measurement of solid electrolyte. The present value, 1.55, is in good agreement with the previously reported value.

The previously reported values of ΔG° and the oxygen partial pressure in equilibrium with MnO and Mn_3O_4 are quoted from Ref. (23–25). The standard Gibbs energy change for reaction (3) is -72.1 ± 0.3 kJ/mol. Taking the activity of MnO of the composition (B_2) to be unity, -75.0 ± 0.3 kJ/mol was obtained. In spite of the small solid solution range, this difference is larger than the experimental error. -73.9, -50.9, and -60.4 kJ/mol are obtained from the previous data of (23), (24) and (25), respectively. Our value is in good agreement with Hahn *et al.* (23)

The Relationship between the Ionic Radius of Lanthanoid and ΔG° Value

The reaction, $\frac{1}{2}Ln_2O_3 + MnO + \frac{1}{4}O_2 = LnMnO_3$, is common in the *Ln*–Mn–O system. The ΔG° values for the reactions versus the ionic radius of lanthanoid elements with 12 coordination in the perovskite structure (26) is shown in Fig. 4. In Fig. 4 the present value is shown together with the previous values which were presented by one of us. Although only four data have been obtained so far, the figure indicates a linear relation between ΔG° and the ionic radius. The same phenomenon at 1273 K was found by Atsumi *et al.* (27).

CONCLUSIONS

(1) A phase equilibrium in the system Sm–Mn–O at 1100°C was established under an oxygen partial pressure from 0 to -13.00 in $\log(P_{O_2}(\text{atm}))$.

(2) Under the present experimental conditions, the Sm_2O_3, MnO, Mn_3O_4, $SmMnO_3$ and $SmMn_2O_5$ phases are stable.

TABLE 4
Lattice Constant of Quenched $SmMn_2O_5$

Sample (mol ratio)						
Sm_2O_3	MnO	Time (h)	a (Å)	b (Å)	c (Å)	V (Å)
0.2	0.8	95.5	7.448 (5)	8.579 (3)	5.686 (2)	363.3 (3)
Ref. (12)		—	7.445 (6)	8.585 (7)	5.68 (4)	363
Ref. (14)		—	7.4332 (7)	8.5972 (7)	5.6956 (5)	363.55 (9)

Note. $SmMn_2O_5$ was prepared at 1100°C in $-\log(P_{O_2}(\text{atm})) = 0.68$.

TABLE 5
Spacing and relative intensities

h	k	l	d (obs.)	d (calc.)	$I/I_0 \times 100$
0	0	1	5.72	5.69	22
0	2	0	4.30	4.29	2
1	1	1	4.008	3.999	2
1	2	0	3.725	3.717	19
1	2	1	3.117	3.111	76
2	1	1	2.930	2.928	100
2	2	0	2.814	2.812	8
1	3	0	2.673	2.670	39
1	1	2	2.542	2.537	25
1	3	1	2.420	2.417	4
0	2	2	2.375	2.370	15
1	2	2	2.262	2.258	11
2	1	2	2.187	2.185	26
1	4	0	2.063	2.061	13
0	4	1	2.009	2.007	15
0	0	3	1.897	1.895	3
3	3	0	1.874	1.875	5
2	4	1	1.767	1.767	5
0	4	2	1.714	1.712	12
2	0	3	1.691	1.689	10
1	4	2	1.670	1.669	5
1	5	1	1.605	1.604	2
4	3	0	1.565	1.560	18
4	1	2	1.531	1.533	3
2	5	1	1.503	1.503	10
3	1	3	1.486	1.484	1
4	2	2	1.465	1.464	2
1	5	2	1.442	1.441	6
0	0	4	1.423	1.422	11
0	1	4	1.405	1.402	5
1	4	3	1.396	1.395	4
0	6	1	1.388	1.387	2
3	3	3	1.333	1.333	4
0	6	2	1.278	1.277	1
3	5	2	1.269	1.264	1
1	3	4	1.256	1.255	7
3	1	4	1.222	1.221	3
2	5	3	1.204	1.204	4

(3) MnO, $SmMnO_3$, and $SmMn_2O_5$ have nonstoichiometric composition. However, Mn_3O_4 is stoichiometric.

TABLE 6
Standard Gibbs Energy Changes of Reaction at 1100°C

Reaction	$-\log P_{O_2}$(atm)	$-\Delta G^\circ$(kJ/mol)
(1) $MnO+\frac{1}{2}Sm_2O_3+\frac{1}{4}O_2 \rightarrow SmMnO_3$	10.00	65.6
(2) $SmMnO_3+\frac{1}{3}Mn_2O_4+\frac{1}{3}O_2 \rightarrow SmMn_2O_5$	1.55	14.2
(3) $3MnO+\frac{1}{2}O_2 \rightarrow Mn_3O_4$	5.40	72.1
	5.62	73.9[a]
	(3.87)	50.9[b]
	(4.60)	60.4[c]

[a] Ref. (23).
[b] Ref. (24).
[c] Ref. (25).

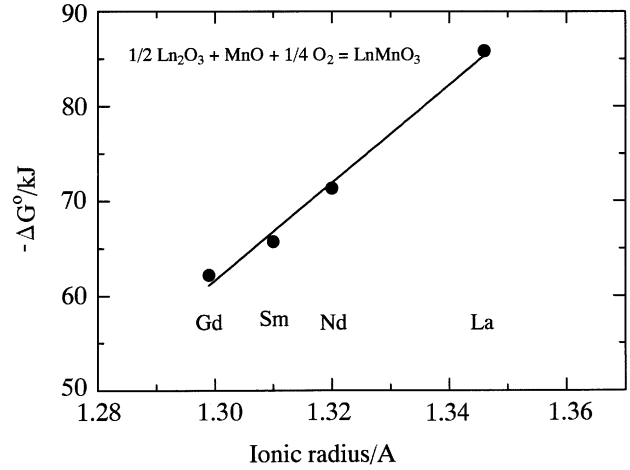

FIG. 4. The ionic radius of lanthanoid element in 12 coordination number versus ΔG° value of the reaction, $\frac{1}{2}Ln_2O_3+MnO+\frac{1}{4}O_2=LnMnO_3$.

(4) Standard Gibbs energies of reactions found in the diagram were calculated with the oxygen partial pressure in equilibrium with three solid phases.

(5) Lattice constants of $SmMnO_3$ and $SmMn_2O_5$, and spacings and relative intensities of $SmMn_2O_5$ were determined.

ACKNOWLEDGMENT

The authors would like to express their sincere gratitude to The Uchida Energy Science Promotion Foundation for lending financial support.

REFERENCES

1. J. B. Goodenough, *Prog. Solid State Chem.* **5,** 149 (1971).
2. C. N. R. Rao, *Annu. Rev. Phys. Chem.* **40,** 291 (1989).
3. B. C. Tofield and W. R. Scott, *J. Solid State Chem.* **10,** 183 (1974).
4. K. Kamata, T. Nakajima, T. Hayashi, and T. Nakamura, *Mater. Res. Bull.* **13,** 49 (1978).
5. T. Nakamura, G. Petzow, and L. J. Gauckler, *Mater. Res. Bull.* **14,** 649 (1979).
6. M. Lucco Borlera and F. Abbattista, *J. Less-Common Met.* **92,** 55 (1983).
7. J. A. M. Van Roosmalen, P. Van Vlaanderen, E. H. P. Cordfunke, W. L. Ijdo, and D. J. W. Ijdo, *J. Solid State Chem.* **114,** 516 (1995).
8. K. Kitayama, *J. Solid State Chem.* **153,** 336 (2000).
9. K. Kitayama and T. Kanzaki, *J. Solid State Chem.* **158,** 236 (2001).
10. K. Kitayama, H. Ohno, R. Ide, K. Satoh, and S. Murakami, *J. Solid State Chem.*, submitted.
11. S, Quezel-Ambrunaz, F. Bertaut, and G. Buisson, *C. R. Acad. Sci. Paris* **258,** 3025 (1964).
12. H. Satoh, S. Suzuki, K. Yamamoto, and N. Kamegashira, *J. Alloys Compd.* **234,** 1 (1996).
13. G. Buisson, *Phys. Stat. Sol.* **17,** 191 (1973).

14. J. A. Alonso, M. T. Casais, M. J. Martinez-Lope, J. L. Martinez, and M. T. Fernandez-Diaz, *J. Phys.: Condens. Matter* **9,** 8515 (1997).
15. H. Nakamura and K. Kohn, *Ferroelectrics* **204,** 107 (1997).
16. K. Kitayama, K. Nojiri, T. Sugihara, and T. Katsura, *J. Solid State Chem.* **56,** 1 (1985).
17. K. Kitayama, *J. Solid State Chem.* **137,** 255 (1998).
18. JCPDS Card No. 25-747.
19. A. Waintal, J. J. Capponi, E. F. Bertaut, M. Contre, and D. Francois, *Solid State Commun.* **4,** 125 (1966).
20. T. Arakawa, A. Yoshida, and J. Shiokawa, *Mater. Res. Bull.* **15,** 269 (1980).
21. R. D. Shannon and C. T. Prewitt, *Acta Crystallogr. B* **25,** 925 (1965).
22. JCPDS Card No. 79-1691.
23. W. C. Hahn, Jr. and A. Muan, *Am. J. Sci.* **258,** 66 (1960).
24. J. F. Elliott and M. Gleiser, "Thermochemistry for Steelmaking," Vol. 1. Addison–Wesley, Reading, MA, 1960.
25. R. A. Robie, R. S. Hemingway, and J. R. Fisher, "Thermodynamic Properties of Minerals and Related Substances at 298.15 K and 1 Bar (10^5 Pascals) Pressure and at Higher Temperatures." Geological Survey Bulletin 1452. United States Government Printing Office, Washington, 1978.
26. G. P. Espinosa, *J. Chem. Phys.* **37,** 2344 (1962).
27. T. Atsumi, T. Ohgushi, and N. Kamegashira, *J. Alloys Compd.* **238,** 35 (1996).